مقاله پژوهشی

لیزرپزشکی؛ ۱۳۸۷، دوره ۵، شماره ۲: صفحات ۵۲-۴۸.

Experimental Studies of Model Drug Delivery Using Superpulse CO_2 Laser

M.E Khosroshahi [1]
Z.S Mansoori [2]
A Jafari Ardebili [2]
M Mahmoodi [1]

[1]Amirkabir University of Technology, Faculty of Biomedical Eng, Biomaterial group, Tehran- Iran

[2]Islamic Azad University (science & research branch), Department of Physics, Tehran- Iran

E-mail:Khosro@aut.ac.ir
Fax: 021-66495655

ABSTRACT

To our knowledge most of the work in the field of drug delivery systems using lasers have been performed using short pulses with micron and submicron durations. We have carried out an experiment using a super long CO_2 laser pulse (10ms) on simulated gelatin-ink model (GIM) .The mechanism of laser- GIM interaction was studied by photothermal deflection and time-resolved dynamics techniques. Energy balance consideration showed a complete non-adiabatic (ie diffusion limit) case with a threshold evaporation intensity of 3.1 $kWCm^{-2}$. The velocity of thermal waves and vaporized plume were measured at below and above ablation threshold as (0.5-2.5) ms^{-1} and (0.4-10) ms^{-1} respectively. The geometry of the modeled tissue at the onset of ablation was semi-spherical but it gradually changed into a cone at later stages whose volume was linearly increased with fluence up to a maximum value of 55 mm^3 at $15kWcm^{-2}$ with drilling velocity of 5.6 cms^{-1} after 20 pulses. We believe that the main mechanism at work with superlong pulses of CO_2 laser is both photothermal due to vaporization and photomechanical due to photophorosis and also cavitation collapse. Thus, drug molecules can be transported into tissue bulk by thermal waves described by the Fick's law in 3-D model for a given cavity geometry and the mechanical waves, unlike only by pure photomechanical waves (ie photoacoustically) as with short pulses.

Key words: Superlong CO_2 Laser, Drug Delivery, Fast Photography, Photothermal Deflection, Conical Cavitation.

INTRODUCTION

Drug delivery systems (DDS) are an area of study in which researchers from almost every scientific discipline can make a significant contribution. Understanding the fate of drugs inside the human body is a high standard classical endeavor, where basic and mathematical analysis can be used to achieve an important practical end. No doubt the effectiveness of drug therapy is closely related to biophysics and physiology of drug movement through tissue.

Therefore, DDS requires an understanding of the characteristics of the system, the molecular mechanisms of drug transport and elimination, particularly at the site of delivery. In the last decade DDS have received much attention since they can significantly improve the therapeutic effects of the drug while minimizing its side effects. In chemical methods, cationic lipids, polymers and liposomes can be used as a drug carrier [1] while physical methods such as high voltage electric pulse [2], CW ultrasound [3], extra corporeal shock wave [4-5], laser induced shock wave [6] have been used as a driving force for drug delivery. In our first report on laser induced cavitation and the role of photoacoustic effects [7] we showed that hot, high-pressure vapor cavity produced at (2.6-3μm) can lead to energy being transported well beyond the laser beam penetration depth as a direct result of the bubble expansion following the pulse and large amplitude acoustic waves associated with bubble formation and decay. Since then much research has been performed on the optical cavitation dynamics [8-10] and potential use of cavitation and photoacoustic as a means of delivering drug into tissue [11-17]. To our knowledge no specific work was found in the literature regarding the dynamic studies of long chopped pulse (τ_p>>ms) CO_2 laser interaction with aqueous solution as a method of drug delivery. With this view we have used fast photography and photothermal deflection techniques to gain an insight about the mechanism of mass and heat transfer into the bulk medium.

MATERIALS AND METHODS

In this study the tissue was modeled using commercial gelatin powder mixed with de-ionized water with weight ratio of 3.5:96.5 formed in a glass cuvett with 20×20×20 mm dimension. The gelatin-water mixture was heated to 60˚C with a magnetic stirrer until it became clear. The drug was simulated using an India blue ink with a high absorption coefficient coated in a thin layer on the gelatin surface. Drug delivery experiments were then performed by using a 30W $C0_2$ laser (SM medical) with 10ms pulse duration in chop-wave mode.

As can be seen in Fig.1 the output of the laser was focused by a l00mm hand piece manipulator into a 500μm spot size on the gelatin surface. Gelatin removal and its absorption coefficient α (cm^{-1})

[Downloaded from icml.ir on 2026-11-03]

measurements were made by exposing the sample to a predetermined number of pulses, n, at pulse repetition frequency of 2Hz and the depth of material removal, Δ, was measured by a resolution optical microscope (Euromex±2μm). The average etch depth was calculated from Δ/n and the slope provided the value of α. The interaction process monitoring system included the time-resolved dynamics of laser- induced cavitation and photothermal deflection at different ablation stages.The first was done by a fast CCD Camera (Panasonic Super Dynamic WV-CP450) connected to an optical microscope (Prior-UK) and for the second method which is PDT, it is known that rapid heating as a result of absorption of laser radiation by a sample generates heat due to various non-radiative excitation processes occurring in the sample which acts as a "thermal piston" driven wave at sound speed. The origin of this wave lies in the heating of air molecules close to the target surface. The heat thus is transferred to the air in the close vicinity of the irradiated surface, resulting in a temperature rise in the surrounding medium. Such a rise in temperature leads to density variations which create a refractive index gradient in the medium adjacent to the surface. A probe beam propagation through this refractive index gradient perpendicular to the direction of the pump beam will suffer refraction and consequently will deviate from its original path. In the PTD experiment the probe beam was a He-Ne laser of 3mW power which after being expanded was focused by a lens of 100mm focal length to a spot diameter of ≤500μm.Deflection of the probe beam was measured as a function of pulse fluence by a fast rising time of 1ns PIN photodiode. The output signal was then recorded by 150MHz digital oscilloscope (Hitachi VC- 7102).

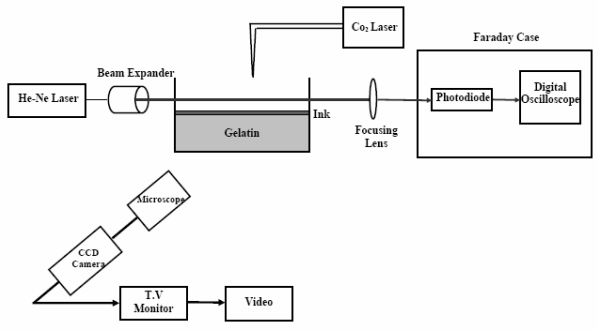


Fig 1-Experimental set up for dynamics studies of laser-gelatin Interaction.

RESULTS AND DISCUSSION

1. Material Removal

Fig 2 shows the etch depth per pulse of gelatin as a function of fluence for the CO_2 laser .It is assumed: (1) the absorption dominant ie $\alpha >> \beta$ where β is the scattering coefficient, (2) ablation commences instantaneously once a threshold fluence F_t is exceeded and (3) if the plume retains the same absorption coefficient as the condensed phase then based on figure 2 one can use the well known Beer-Lambert's law to describe the etch depth rate fluence dependences.

$$h = \alpha^{-1} \ln (F / F_t) \qquad (1)$$

Where h and F are etch depth per pulse and fluence respectively. A fit to the data using equation (1) yields $F_t \approx 32$ Jcm^{-2} (ie≈ 6.2W) which is in agreement with the theoretical value given by the energy balance for threshold evaporation intensity, $I_t \approx 3.1$ $kWcm^{-2}$.

$$I_t = (\rho_g . L_V . d_0) / \tau_p \qquad (2)$$

Where $\rho_g \approx 1.2$ gcm^{-2} is the density of gelatin, $L_V \approx 2.260$ kJ/g is the latent heat of vaporization of water, $d_0 \approx \alpha^{-1} \approx 116\mu m$ is the optical penetration depth of CO_2 laser radiation in gelatin, where α is determined from the inverse slope in Fig 2 as $86cm^{-1}$ and $\tau_p = 10$ ms is the pulse duration.

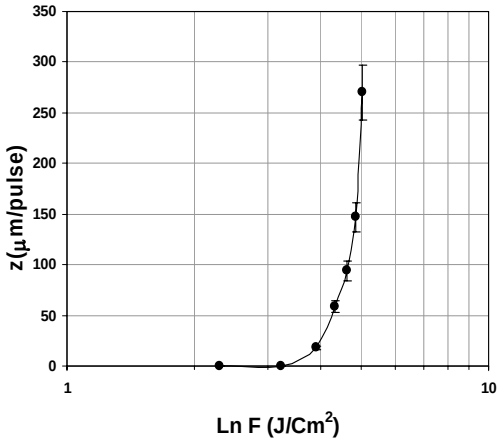


Fig 2- Ablation depth per pulse of GIM versus fluence

2. PTD Analysis

By assuming a Gaussian profile for the probe beam, one can write the dependence of the photodiode response ΔV on the beam deflection as follows [18]:

$$\Delta V = V_0 \, erf [\sqrt{2} \, \varphi / \theta] \qquad (3)$$

With φ and θ being the beam angular deflection due to change in index of refraction and angular divergence respectively, V_0 is the photodiode output voltage at φ=0, erf is the complementary error function ie:

$$erf(x) = 2 / \sqrt{\pi} \int_0^x \exp(-t^2) dt \qquad (4)$$

Therefore only for $\varphi << \theta$, ΔV is linear. Fig 3 shows the output voltage (hence deflection) as a function of laser fluence. It can be seen that the voltage amplitude increases linearly with fluence which defines the origin of the signals observed. Fig 4a indicates that below the ablation threshold the bipolar deflection is mainly caused by thermal piston effect (ie. A pressure wave)

[Downloaded from icml.ir on 2026-11-03]

which is generated by hot surface. Since the refractive index of the gelatin increases with density, so that the probe deflects towards the higher or positive density region and later times it is followed by a negative lobe which is thought to be produced by the mixture of convective plume of the gaseous air and relaxation of the probe beam. In our experiment the probe-surface distance was≈1mm which gives a velocity profile of (0.5-2.5) m/s at 30Jcm^{-2} whereas in Fig.4b this corresponds to (0.4-10) m/s at 125Jcm^{-2} .It must be noted that at fluences well above threshold, the compressive uni-polar deflection is due to the ablated hot particulates from the target surface.

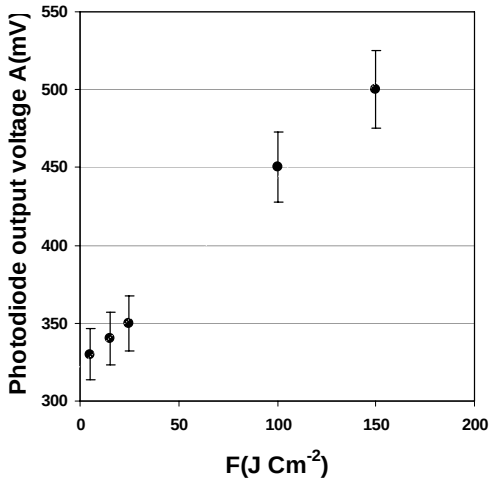


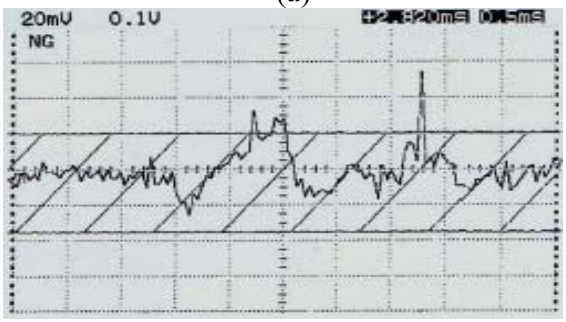
Fig 3- Photdiode output signal as a function of fluence

Therefore, the distribution of heat and mass transfer in Fig- 4b shows an hybrid multimode structure or hotspots which is an irregular beam profile resulting in inhomogeneous heating and vaporization of gelatin volume. To visualize these irregularities in two-dimension profile, the He-Ne laser was scanned above the surface (Fig .5a) and just below the gelatin surface (Fig.5b), in an ablative regime.

The nature of the bubble motion (photophoresis) is explained by the temperature gradient in irradiated liquid. The propulsion force acting on the bubble arises from the difference in the surface tension on the irradiated and non-irradiated side of the bubble. It is the tendency of the liquid to flow into the region with higher tension coefficient making the bubbles move towards the source of heating. It is believed that the Archimedes force tends to drive the bubbles from the laser heated zone to the somewhat above the probe beam. The pattern of the scattered beam changes, as the probe beam suffers total internal reflection on the spherical bubbles surface and thus is deflected downwards. Brighter portions of the cavity represent the greater bubble density which trap the light as bubbles move upwards just beneath the surface. The time resolved studies related to these phenomena is discussed in the next section.

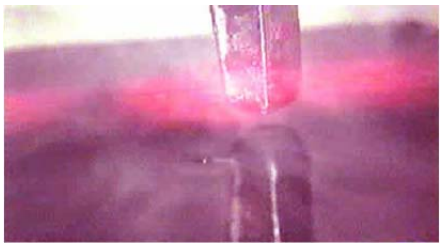


(a)

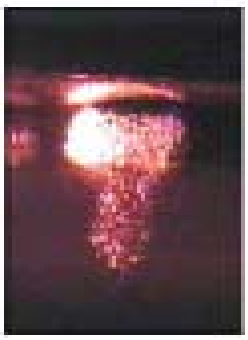


(b)

Fig 4- Photothermal deflection signals below (a) and above (b)ablation threshold of gelatin.



(a)



(b)

Fig 5- (a) vaporized material visualized above the gelatin surface at P= 15W, (b) Trapped probe beam by the bubbles of the cavity at P = 30W

3. CAVITY DYNAMICS

In order to get an insight about the mechanism of cavity formation and possible delivery of drug into a tissue the ablation process of GIM at different laser power was photographed by a CCD camera and then suitably captured.

As it can be seen from Fig 6, the geometry of cavities after 20 pulses somewhat varies with power

[Downloaded from icml.ir on 2026-11-03]

level and exhibited a non-linear behaviour with a conical shape in general.

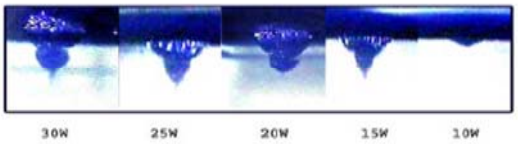


Fig 6- laser–induced cavitation geometry at different Laser powers

As an example, the variation of cavity diameter with laser pulse numbers in Fig 7 indicates that the diameter of upper portion (D) and lower portion (d) of cavities in fig.6 both initially increase and after the tenth pulse reach the saturation point. It is interesting to note that the cavity diameters increase with increasing the fluence. Also, the total cavity depth due to vaporization and the hydrodynamic flow resulting from the bubbles which act as a driving thermo-mechanical force can be studied in terms of laser pulse numbers. It is clear from Fig.8 that the largest depth achieved in this experiment was about 5.5 mm at 150 Jcm^{-2}. It is important to notice that there exists a limiting value of depth as an harmonic and reproducible behaviour after saturation point for every values of fluences.

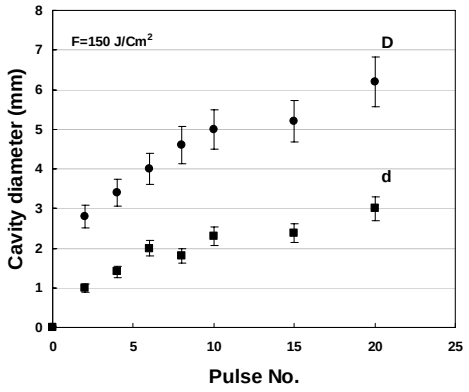


Fig7- Diameter of upper (D) and lower (d) portions of cavity as a function of laser pulse number

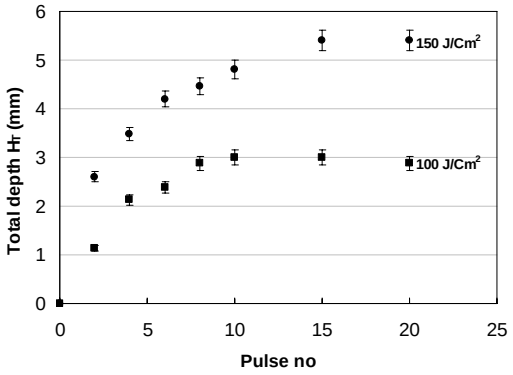


Fig 8- Total depth of cavity measured at different fluences

Finally, the total volume of cavities shown in Fig 5 is plotted as a function of power density, Fig 9. A volume of ≈50 mm^3 can be produced by 20 laser pulses at 15kWcm^{-2}. Of course, macroscopic flow of material from one phase to another is possible at equilibrium. Hence, to maintain a strong evaporation, a certain overheating of the condensed phase is necessary. Therefore, the knowledge of drilling or thermal evaporation velocity, $\dot{Z}_T$, can be helpful to determine the dependence of temperature (T) on intensity (I) and the pressure at condensed phase (P_c) using the relation:

$$P_c = P_g + [\ \rho_c . \dot{Z}_T . V_g\ ] \quad (5)$$

Where P_g is the pressure at gaseous phase, ρ_c is the density of gelatin at condensed phase, V_g the velocity of molecules, and

$$\dot{z}_T = I/\ \rho_c . L_v \quad (6)$$

Using equation (6) gives a value of ≈1.1cm/s at threshold power of 3.1kWcm^{-2} and 5.6cm/s at 15kWcm^{-2} respectively. The major part of the energy needed to evaporate organic materials such as biological soft tissues with a onsiderable water content is consumed by the phase change of the contained water. Thus for gelatin and most soft tissues, the ratio $I/\dot{z}_T$ will be essentially determined by the water content in (gcm^3).

During the drilling process, a liquid layer is present between the gaseous and the condensed phase. By the action of the existing pressure gradient, the liquid is pushed towards the origin of low pressure. Therefore, liquid material will be driven in radial direction towards the wall of the cavity and then escapes along this wall from the evaporation wave front.

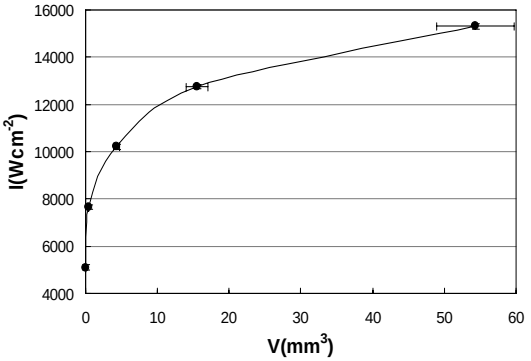


Fig 9- Corresponding volume of cavities produced at given laser power densities

In summary, a conical shape crater with a total depth of 5.5 mm and a diameter of 6 mm was produced in the gelatin after 20 pulses at 150 Jcm^{-2} with a drilling velocity of 5.6cms^{-1}. The corresponding volume under these conditions was about 55 mm^3. We believe that the main operating mechanism with super long CO_2 laser where the absorption coefficient of GIM is high, is due to combined effects of photothermal because of vaporization and photomechanical because of photophorosis and cavitation collapse, unlike only due to photomechanical (ie photoacoustical) effect as had previously been reported. Therefore, provided the drug is not completely vaporized and tissue is not damaged in anyway, then the drug molecules can be transported into tissue bulk described by the Fick's law in conical

[Downloaded from icml.ir on 2026-11-03]

geometry and mechanical waves. Our next work is acoustic pressure measurement induced by the collapse of these bubbles at long delayed time and thermodynamic analysis of drug molecules transportation.

References

1. Konan Y, Gulny R, J.photochem. Photobiol. B, 2002; 66: 89.
2. Rivlere J, Heit M, Pharm.Res. 1997; 14: 687.
3. Tachibana K, Tachibana S. Jpn J Phys 1999; 38: 3014.
4. Gambihler S, Delius M. Naturwissenschaften. 1992; 79: 328.
5. Kodama T, Hamblin M, Doukas A. Cytoplasmic molecular delivery with shock waves. Biophysical J 2000; 79: 1821.
6. Ogura M, Sato S, Terakawa M, et al. Delivery of photosensitizer to cells by the stress wave induced by a single nanosecond laser pulse. Jpn J Appl Phys 2003; 42: 1-977.
7. Dyer P.E, Khosroshahi M.E, Tuft S. Studies of laser- induced cavitation and tissue ablation in salin using a fiber-delivered pulsed HF laser. Appl Phys B 1993; 56: 84.
8. Asshauer T, Delacretz G. Acoustic transients in pulsed holmium laser ablation. SPIE 1994; 2323: 117.
9. Palanker D, Turovets I, Lewis A. Dynamics of ArF excimer laser-induced cavitation bubbles in gel surrounded by a liquid medium. Lasers in Med 1997; 21: 294.
10. Frenz M, Konz F, Pratisto H. Starting mechanisms and dynamics of bubble formation induced by Ho: YAG laser in water. J Appl Phys 1998; 84: 5905.
11. Shangguan H, Casperson L, Shearin A, Prahl S. Investigation of cavitation bubble dynamics using particle image velocimetry: implications of photoacoustic drug delivery. SPIE 1997; 2671: 104.
12. Shangguan H, Casperson L, Shearin A. Prahl Drug delivery with microsecond laser pulses into gelatin. Appl Opt 1996; 35: 3347.
13. Kodama T, Hamblin M, Doukas A. Cytoplasmic molecular delivery with shock waves. Biophysical J 2000; 79: 1821.
14. Shangguan H, Casperson L, Shearin A, Prahl S. Enhanced laser thermbolysis with photomechanical drug delivery. Laser in Surg Med 1998; 23: 151.
15. Singh R, Kim W, Ollinger M, et al. Laser based synthesis of nanofunctionalized particulates for pulmonary based controlled drug delivery application. Appl Sur Su Controlled drug delivery applications. Appl Sur Su 2002; 197: 610.
16. Mandellis A, Baddour N, Cai Y, Walmsley R. Laser-induced photothermoacoustic pressure-wave pulses in a polystyrene well and water system used for photomechanical drug delivery. JOSA B 2000; 22: 1024.
17. Menezes V, Takayama K, Ohki T, Go palan J. Laser–ablation assisted microparticles acceleration for drug delivery. Appl Phys Lett 2005; 87.
18. Diaci J, Mozina J. A study of blast waveforms detected simultaneously by a microphone and a laser probe during laser ablation of metals. J Appl Phys A 1992; 55: 84.

[Downloaded from icml.ir on 2026-11-03]